Thermal response of energy foundations installed in unsaturated residual soils

Michael B. Reiter[1], *Thaise da S. O.* Morais[2], *Cristina de H.C.* Tsuha[2], and *Tugce* Baser[1,*]

[1]University of Illinois at Urbana Champaign, Department of Civil and Environmental Engineering, USA
[2]University of São Paulo at São Carlos, Department of Geotechnical Engineering, Brazil

Abstract. This study focuses on the thermal response of energy foundations with different piping geometries installed in unsaturated soil. Energy foundations are an efficient alternative to traditional space heating and cooling approaches and can reduce energy demand for air conditioning in Brazil, where unsaturated residual soil deposits are abundant. A three-dimensional numerical model for heat transfer and subsurface flow is first validated against field data from a thermal response test at the University of São Paulo. The model is then used to compare the performance of triple and quadruple U-tube piping geometries and helical piping geometries of equivalent length. The helical geometries resulted in initial less uniformly heated foundations and lower heat flux at the foundation boundary compared with the U-tubes, but the differences between the U-tube geometries and their equivalent length helices were less than 1°C. All piping geometries exhibited increased heat output as the length of heat exchanger piping increased. The infinite line source solution was compared with the model results. The infinite line source solution underestimated the thermal response of the system during the first 25-30 days and overestimated it afterwards.

1 Introduction

Heating and cooling buildings consumes a large quantity of electricity that is often sourced from fossil fuels across the world. In tropical countries like Brazil, cooling demand is dominant. Electricity consumption due to traditional air conditioning systems is significant and it comprises an important part of the national electricity demand. Shallow geothermal energy technologies such as energy foundations can provide high rates of energy efficiency and are sustainable alternatives to conventional air-source heat pumps [1], and can reduce the energy consumption.

Energy foundations exchange heat between structural elements of foundations and surrounding soil for heating and cooling of buildings. They function by circulating a fluid through polyethylene pipes installed with different configurations within foundations, including U-tube and helical configurations. Different piping geometries exhibit different heat transfer efficiencies but require variable effort during installation. Installation of a helical piping geometry may be more laborious than a U-tube geometry.

Unlike USA and most countries in Europe, installation of energy foundations is new in Brazil where unsaturated residual soils are widespread. Therefore, a better understanding of the performance of energy foundations in such soils is required for efficient design and development of guidelines. The main objective of this study is to investigate the differences in heat transfer efficiency between four pipe geometries in an energy foundation installed in a residual unsaturated soil profile on the São Carlos campus of University of São Paulo, Brazil. First, the results from a field-scale Thermal Response Test (TRT) were used to validate a numerical model, then the model was used to simulate thermal response of the piles for 35 days and the results were compared against a widely used analytical solution.

2 Background

Heat transfer in unsaturated soils can be complex because of the presence of multiple fluid phases and the coupled behavior of thermal and hydraulic processes. Taylor and Cavazza [2] performed laboratory scale experiments in which temperature gradients were imposed on unsaturated silt to observe flow of water vapor from warm to cool regions accompanied by a return flow of liquid water from cool to warm regions. They attributed the vapor flow to convection of air and diffusion of vapor, while the reverse liquid water flow was attributed to the pressure gradient induced by the condensation of vapor in the cooler regions. Philip and de Vries [3] formulated the coupled heat transfer and liquid water and vapor flow in unsaturated porous materials based on those driving forces. They found that water transfer is low in very dry or very wet media and maximized at some intermediate water content. [3] also noted significant latent heat transfer by vapor condensation in soils at intermediate water contents.

Another component that govern heat transfer and water flow in unsaturated soils is the interdependence of

* Corresponding author: tbaser@illinois.edu

relevant soil thermal and hydraulic properties. Thermal conductivity and specific heat capacity are dependent on the degree of saturation, while the soil water retention curve and hydraulic conductivity function are dependent on temperature [4,5]. Baser et al. [6] and Baser and McCartney [7] investigated the role of coupled heat and moisture transfer in unsaturated soils in the context of shallow geothermal systems through numerical analysis, tank-scale experiments, and full scale field-scale experiments and concluded that consideration of coupled thermal and hydraulic material properties and heat transfer mechanisms was important.

The efficiencies of different heat exchanger pipe geometries in energy foundations have been studied by several researchers. Gao et al. [8] performed field-scale experiments and numerical analyses on energy foundations with four different heat exchanger piping geometries installed in Shanghai, China including a single W-loop and single, double, and triple U-tubes in parallel. They reported that the W-loop had the highest heat transfer performance. Zarella et al. [9] compared the thermal response of helical and triple U-tube geometries in an energy foundation via numerical analyses based on analogical resistance circuits and validated the numerical model with full-scale field measurements. They concluded that the helical configuration provided better performance than the U-tube and that the performance increased with decreasing helix pitch. Bezyan et al. [10] used three-dimensional finite element numerical analyses to simulate the thermal response of U-tube, W-loop, and helix piping geometries. They simulated the pipe geometries in series and in parallel and compared several helix pitches, concluding that the helix had the highest heat transfer and that in-series pipe configurations transferred more heat than in-parallel configurations. [11] also found that a maximum heat transfer rate was achieved at some ideal helix pitch length, beyond which heat transfer decreased. Park et al. [11] evaluated the thermal response of W-loop and triple U-tube in series geometries in foundations in unsaturated weathered granite in Korea using a numerical model and field-scale experiments and they reported higher heat transfer rates from the U-tube compared to the W-loop during intermittent operation, but negligible difference during long-term, continuous operation.

3 Model Description

In this study, a three-dimensional finite element model is used to simulate the transient thermal responses of the heat exchanger fluid, concrete, and surrounding soil. Heat transfer in the circulation fluid, concrete, and soil are coupled with water flow in unsaturated porous media. The coupled system of equations is solved using COMSOL Multiphysics v5.4b.

3.1 Formulation

Heat transfer in the circulation fluid is described as follows:

$$\rho_f A C_{p,f} \frac{\partial T_f}{\partial t} + \rho_f A C_{p,f} u \boldsymbol{e_t} \cdot \nabla T_f = \nabla \cdot \left(A k_f \nabla T_f\right) + \frac{1}{2} f \frac{\rho_f A}{d} |u| u^2 + Q_{wall} \quad (1)$$

where ρ_f is the density of the circulation fluid (kg/m^3), A is the cross-sectional area of flow (m^2), $C_{p,f}$ is the specific heat capacity of the fluid (J/kgK), T_f is the fluid temperature (K), u is the flow velocity (m/s), $\boldsymbol{e_t}$ is a unit vector tangent to the direction of flow, k_f is the thermal conductivity of the fluid (W/mK), d is the internal diameter of the pipe (m), and f is a pipe friction factor that is a function of the specific roughness of the pipe material e (m) [11]. Q_{wall} describes the transfer of heat across the pipe wall and is expressed as follows:

$$Q_{wall} = hZ(T_{ext} - T_f) \quad (2)$$

where h is an effective heat transfer coefficient (W/m^{2}K), Z is the effective perimeter of the pipe wall (m), and T_{ext} is the temperature external to the pipe (°C). The effective heat transfer coefficient is a function of the thermal conductivity of the pipe material λ_w (W/mK) and pipe wall thickness b (m) [12]. Pipe flow is assumed to be one-dimensional and fully developed along a linear element with constant velocity.

Heat transfer in the unsaturated soil is expressed including convection in the fluid phase and conduction in the solid phase as follows:

$$\rho C_p \frac{\partial T}{\partial t} + \rho_w C_{p,w} \boldsymbol{u} \cdot \nabla T = \nabla \cdot (\lambda \nabla T) \quad (3)$$

where ρ is the density of the soil (kg/m^3), C_p is the specific heat capacity of the soil (J/kgK), ρ_w is the density of the pore fluid (kg/m^3), $C_{p,w}$ is the specific heat capacity of the pore fluid (J/kgK), $\boldsymbol{u}$ is the pore fluid velocity vector (m/s), T is the temperature (K), and λ is the thermal conductivity of the soil (W/mK). The apparent density, thermal conductivity, and specific heat capacity of the soil matrix are calculated by volume averaging the constituent values for the soil solid and pore water via the porosity n. Equation 3 is also applied to the concrete foundation with separate material parameters and the fluid velocity term equal to zero. Subsurface flow through the porous matrix is described as:

$$n \frac{dS_r}{dP_c} \frac{\partial (\rho_w P_c)}{\partial t} + \nabla \cdot \boldsymbol{u} = 0 \quad (4)$$

where **u** is the Darcy velocity vector and is expressed as follows:

$$\boldsymbol{u} = -\frac{\kappa \rho_w}{\mu} (\nabla p_w + \rho_w g \nabla z) \quad (5)$$

μ is the fluid dynamic viscosity (Pa s), p_w is the pore water pressure (Pa), and g is gravitational acceleration (m^2/s). The degree of saturation S_r and intrinsic permeability κ (m^2) are based on the van Genuchten [13] and Mualem [14] models for the soil water retention curve and hydraulic conductivity function:

$$S_r = S_{res} + (1 - S_{res})[1 + \alpha P_c)^N]^{-(1-1/N)} \quad (6)$$

where S_{res} is the residual degree of saturation, α (1/Pa) and N are fitting parameters, and P_c is the capillary pressure

(Pa), equal to the difference between the pore gas pressure and the pore water pressure. In this analysis the pore gas pressure is set to zero. Finally:

$$\kappa = \frac{\mu k_s}{\rho_w g} S_e \left[1 - (1 - S_e^{N/(N-1)})^{N/(N-1)}\right]^2 \quad (7)$$

where k_s is the saturated hydraulic conductivity (m/s), and S_e is the effective degree of saturation expressed as follows:

$$S_e = {S - S_{res}}/{1 - S_{res}} \quad (8)$$

3.2 Validation

To validate the numerical model, a full-scale thermal response test (TRT) performed on an energy foundation with a single U-tube heat exchanger on the São Paulo campus of University of São Paulo, Brazil by Morais and Tsuha [15] was used. The subsurface profile in the area is predominantly comprised of clayey sand with a silty sand layer atop. The groundwater table fluctuates seasonally between 2 and 3 m from the surface at the test site. The overall thermal conductivity of the saturated clayey sand was found to be 2.8 W/mK which is consistent with the values for saturated sands exist in the literature [4].

The geometry and initial and boundary conditions of the numerical model match those in the field scale TRT. Only the top 1.9 m of the soil column was unsaturated, but the case study was used for validation because it was performed locally. The model geometry is shown in Figure 1(a) and 1(b).

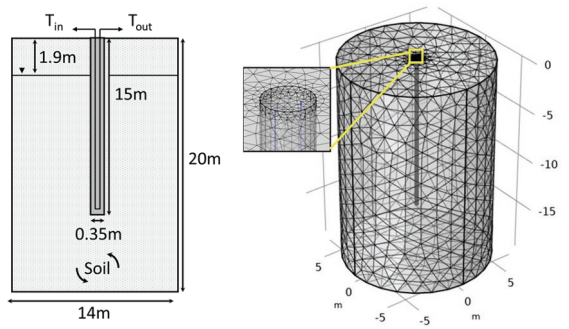

(a) (b)

Fig. 1. Schematic (a) and mesh (b) for replication of [14].

An initial temperature of 24.7 °C and initial hydrostatic pressure distribution with groundwater at a depth of 1.9 m were applied. A temperature of 24.7 °C was maintained on the bottom and lateral exterior boundaries of the soil domain and a temperature of 28.35 °C was maintained at the top of the soil domain. For subsurface flow, a "no-flow" Neumann-type boundary was applied to the exterior boundaries and foundation-soil interface. The inlet temperature time series reported by Morais and Tsuha [15] was digitized and applied to the inlet as a boundary condition. The back-calculated thermal conductivity of the soil from Morais and Tsuha [15] was used as an input parameter. Other input parameters of the numerical model are shown in Table 1.

Table 1. Input parameters for model validation

Parameter	Value	Units
Heat Exchanger Fluid Flow rate, V_f	3.52x10^{-4}	m^3 s^{-1}
Heat Exchanger Pipe Inner Diameter, d	26	mm
Heat Exchanger Pipe Wall Thickness, b	3	mm
Thermal Conductivity of the Heat Exchanger Pipe Wall, λ_w	0.5	W m^{-1} K^{-1}
Thermal Conductivity of the Concrete, λ_c	2.0	W m^{-1} K^{-1}
Effective Thermal Conductivity of the Soil, λ_s	2.8	W m^{-1} K^{-1}
Density of the Concrete, ρ_c	2,400	kg m^{-3}
Density of the Soil Solids, ρ_s	2,700	kg m^{-3}
Heat Capacity of the Concrete, $C_{p,c}$	900	J kg^{-1} K^{-1}
Heat Capacity of the Soil, $C_{p,s}$	900	J kg^{-1} K^{-1}
Soil Porosity	0.50	--
Soil Saturated Hydraulic Conductivity, K_s	1x10^{-5}	m/s
vG Air Entry Suction Fitting Parameter, α	1.49	kPa^{-1}
vG Pore Size Distribution Fitting Parameter, N	1.20	--
Residual Water Content	0.05	--
Pipe surface roughness, e	0.0015	mm

The results from the simulation and the published results are shown in Figure 2. The outlet temperatures from the model and the reported outlet temperatures from the field are within 1°C.

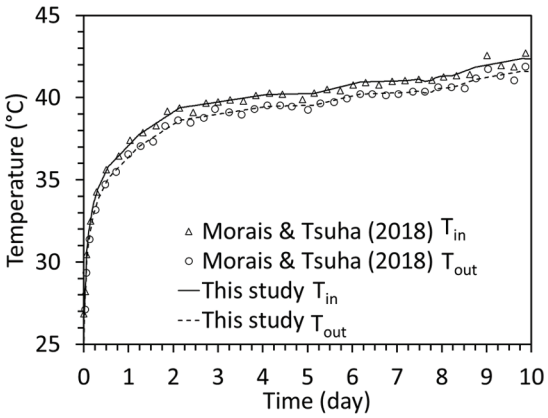

Fig. 2. Inlet and outlet temperatures from [14] and this study.

4 Comparison of helical and U-tube pipes

4.1 Geometry

The numerical model was used to compare the thermal response of energy foundations in unsaturated soils with four different piping geometries: (1) triple U-tube in series, (2) a helix with length equivalent to the triple U-tube geometry, (3) quadruple U-tube in series, and (4) a helix with length equivalent to the quadruple U-tube

geometry. The simulated pipe geometries are shown in Figure 3. The dimensions of the foundation and the pipes are representative of a bored single U-tube energy pile constructed in 2014 at the test site of São Carlos campus of the University of São Paulo.

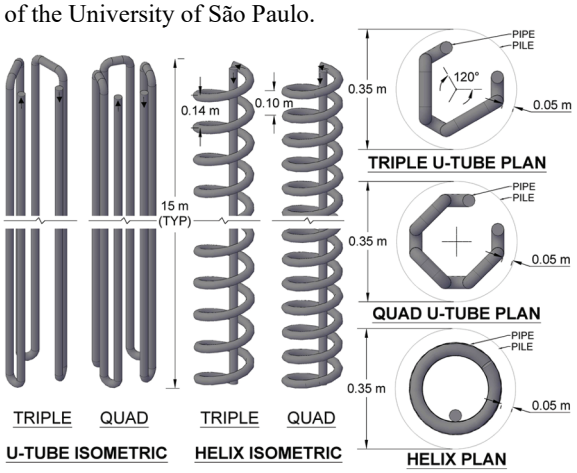

Fig. 3. Simulated heat exchanger piping geometries.

The simulated geometry of the foundation having different pipe configurations and soil domain are shown in Figure 4(a) and 4(b). The depth of the soil column below the foundation and lateral extent of the soil around the foundation were selected to eliminate interaction with the boundaries and optimize model computation time. COMSOL's physics-based free tetrahedral meshing scheme was utilized, with the mesh size varying from extra fine (0.03 m to 0.7 m element size) at the inner foundation domain to fine (0.2 m to 1.6 m element size) at the edge of the outer soil domain. Each model was comprised of up to 350,000 degrees of freedom.

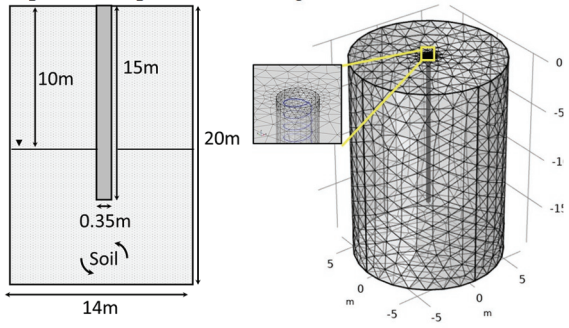

Fig. 4. Schematic (a) and mesh (b) for the comparison of helical and U-tube geometries

4.2 Initial and boundary conditions

An initial temperature of 25.2°C and initial hydrostatic pressure distribution with groundwater at a depth of 10 m were applied. The initial temperature is fixed at all external boundaries throughout the analysis. For subsurface flow, a "no flow" Neumann boundary condition is applied at the external boundaries. The fluid temperature at the inlet is maintained constant at 40°C.

The input parameters for the analysis are shown in Table 2. COMSOL's built-in temperature- and pressure-dependent relations for liquid water were used to define fluid viscosity, density, and thermal properties.

Table 2. COMSOL input parameters.

Parameter	Value	Units
Heat Exchanger Fluid Flow rate, V_f	20	L min^{-1}
Heat Exchanger Pipe Inner Diameter, d	2.6	cm
Heat Exchanger Pipe Wall Thickness, b	3	mm
Thermal Conductivity of the Heat Exchanger Pipe Wall, λ_w	0.5	W m^{-1} K^{-1}
Thermal Conductivity of the Concrete, λ_c	1.5	W m^{-1} K^{-1}
Effective Thermal Conductivity of the Soil, λ_s	1.0	W m^{-1} K^{-1}
Density of the Concrete, ρ_c	2,400	kg m^{-3}
Density of the Soil Solids, ρ_s	2,700	kg m^{-3}
Heat Capacity of the Concrete, $c_{p,c}$	900	J kg^{-1} K^{-1}
Heat Capacity of the Soil Solids, $c_{p,s}$	900	J kg^{-1} K^{-1}
Soil Porosity	0.50	--
Soil Saturated Hydraulic Conductivity, K_s	10^{-5}	m/s
van Genuchten Air Entry Suction Fitting Parameter, α	1.49	kPa^{-1}
van Genuchten Pore Size Distribution Fitting Parameter, N	1.20	--
Residual Water Content	5	%
Pipe surface roughness, e	0.0015	mm

5 Analysis and results

Temperature profiles at the axis of the foundation are shown in Figure 5 for the triple U-tube and equivalent length helix geometries. The difference between the two geometries is less than 0.5°C after one day and decreases with time. The U-tube is more efficient at heating the foundation uniformly with depth. The helical geometry results in a lower temperature at the top of the foundation and a higher temperature at the bottom.

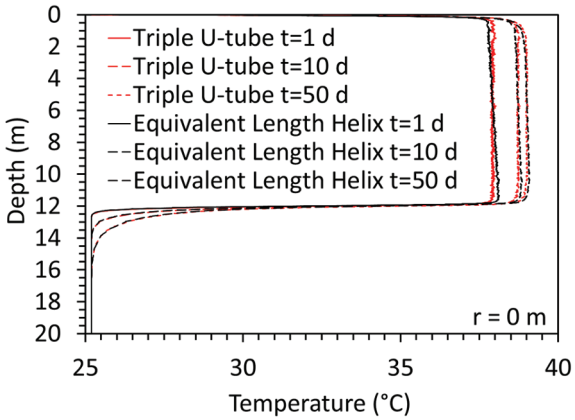

Fig. 5. Temperature at pile axis for triple U-tube and helix

Temperature profiles at the axis of the foundation for the quadruple U-tube and equivalent length helix are shown in Figure 6.

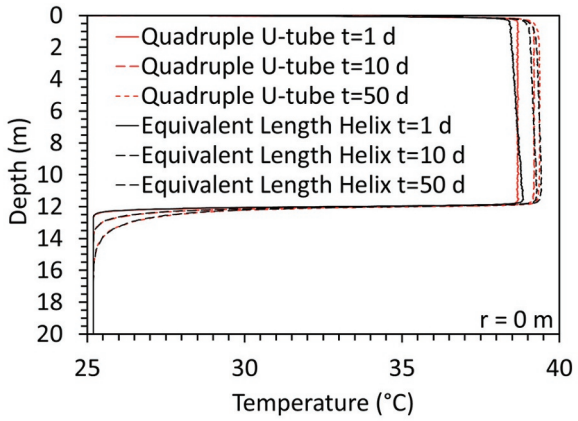

Fig. 6. Temperature at pile axis for quadruple U-tube and helix

The temperature within the pile in the case of the quadruple U-tube and helix pipes were approximately 1 °C higher than the triple U-tube and helix after one day, but the difference decreases with time. The temperature distribution from U-tube was uniform than the helix, but the temperatures are within 0.5°C after one day and the difference decreases with time.

The heat flux integrated over the boundaries of the foundations is shown in Figure 7 for each geometry to eliminate the effect of pipe configuration at the pile walls. The flux is slightly higher for the U-tubes than the equivalent length helices. The heat flux from the quadruple U-tube is approximately 15 watts greater than the flux from both the equivalent length helix and the triple U-tube geometry. The total energy flux from the triple T-tube geometry is 15 watts greater than the equivalent length helix. The heat output from the helix with length equivalent to the quadruple U-tube is nearly equivalent to the output from the triple U-tube. Additional pipe length results in higher heat flux in all cases.

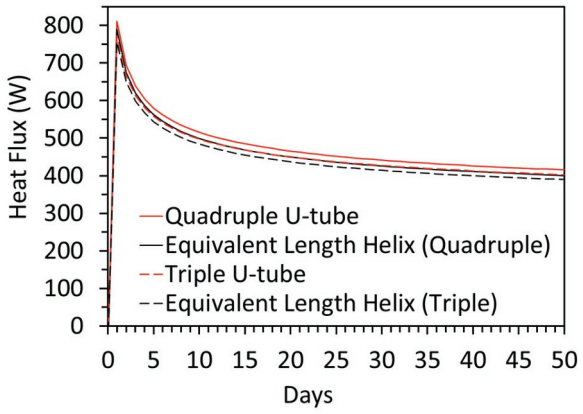

Fig. 7. Total energy flux integrated over the foundation boundary for each geometry.

The fluxes shown in Figure 7 were used to back calculate the temperature at the foundation boundary using the Infinite Line Source (ILS) model using equation 9 as follows:

$$T(r_b,t) = T_0 + \frac{q}{4\pi k_s}\left[\ln\left(\frac{4\alpha t}{r_b^2} - \gamma\right)\right] \; for \; \frac{\alpha t}{r_b^2} \geq 5 \qquad (9)$$

where T_0 is the undisturbed initial temperature (°C), q is the heat flux per unit length of the heat source (W/m), α is the ground thermal diffusivity (m^2/s), r_b is the radius of the foundation (m), and γ is Euler's constant. Although a typical TRT lasts less than the total simulated time in this study, the results are not affected by the duration of heating as the steady state temperatures converge. The results are compared with the simulated average temperatures in Figure 8 for the triple U-tube and equivalent-length helix geometries. The temperatures from the numerical model and ILS solution were different until heating reached 25 days.

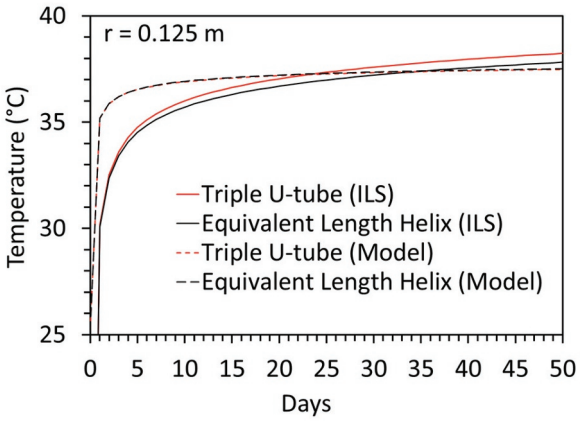

Fig. 8. Temperatures at pile radius from ILS and model (triple U-tube geometry)

The results from the quadruple U-tube and equivalent-length helix geometries are shown in Figure 9. For the first 25-30 days, the temperature is underestimated by the analytical solution. Afterwards, the temperature is overestimated by the analytical solution. The U-tube geometries have higher heat flux at the foundation boundary, which causes the infinite line source to predict a temperature difference of about one degree, but there is no difference between the boundary temperatures from the numerical model.

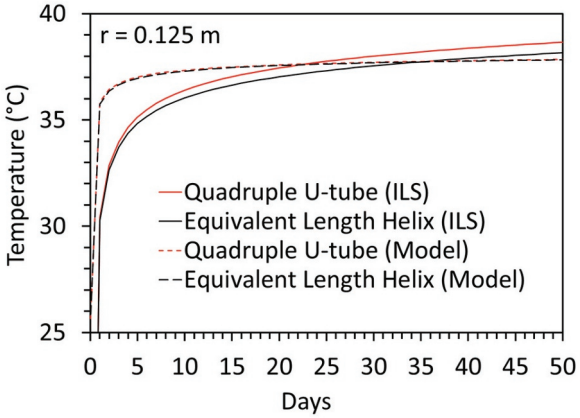

Fig. 9. Temperatures at pile radius from ILS and model (quadruple U-tube geometry)

6 Discussion

Based on the results of this study, the heat transfer efficiency of an energy foundation piping geometry is affected by the total length of heat exchanger piping installed and less affected by the geometry itself. The helical geometries resulted in less uniformly heated foundations and lower heat flux at the foundation boundary compared with the U-tube, but the differences between the U-tube geometries and their equivalent length helices were less than 1°C. These results suggest that increased heat efficiencies observed by others in helical pipe configuration may actually be associated with increased pipe length [e.g., 9,10]. Differences in thermal response between the four geometries peaked at early times and temperatures became more similar as time passed. In general, the ILS analytical solution was within approximately 3 °C of the modeled temperatures after the first 5-10 days. The ILS underestimated the response in the first 25-30 days and overestimated it afterwards. This inaccuracy can be attributed to the thermal inertia of the foundation, the differences in material properties between the foundation and the soil, and the geometry of the heat exchanger piping. None of these factors are considered in the ILS solution.

7 Conclusions

In this study, the thermal response of an energy foundation in unsaturated soil with four different heat exchanger pipe geometries was investigated. The main conclusions drawn from this study are as follows:

- Temperatures at the foundation axis were within 0.5°C between the triple or quadruple U-tube geometries and their equivalent length helical geometries. Differences were highest at early times and decreased as the analysis progressed. The U-tube geometries resulted in a more uniformly heated foundation than the helical geometries.
- Heat flux across the foundation boundary was higher for the U-tubes than the equivalent length helices. The flux from the U-tube geometries were approximately 15 watts greater than the flux from their respective equivalent length helices. Additional pipe length resulted in higher heat flux for both helical and U-tube geometries.
- The ILS analytical solution underestimated the temperature at the foundation boundary during the first 25-30 days and overestimated the temperature at later times.

Financial support provided by the Lemann Faculty Collaborative Research Grants at University of Illinois at Urbana Champaign, the State of São Paulo Research Foundation - FAPESP (Process 2014/14496-0), and the National Council for Scientific and Technological Development - CNPQ (Process 140143/2015-7 and 310881/2018-8) are greatly appreciated. The opinions are those of the authors alone and do not reflect the viewpoint of the sponsors.

References

[1] M.A. Omer, Ground-source heat pumps systems and applications, Renewable and Sustainable Energy Reviews. 12 (2008) 344–371. https://doi.org/10.1016/j.rser.2006.10.003.

[2] S.A. Taylor, L. Cavazza, The movement of soil moisture in response to temperature gradients 1, Soil Science Society of America Journal. 18 (1954) 351–358. https://doi.org/10.2136/sssaj1954.03615995001800040001x.

[3] J.R. Philip, D.A.D. Vries, Moisture movement in porous materials under temperature gradients, Eos, Transactions American Geophysical Union. 38 (1957) 222–232. https://doi.org/10.1029/TR038i002p00222.

[4] O.T. Farouki, The thermal properties of soils in cold regions, 1981. http://www.sciencedirect.com/science/article/pii/0165232X81900410 (accessed March 31, 2019).

[5] N. Lu, Y. Dong, Closed-form equation for thermal conductivity of unsaturated soils at room temperature, Journal of Geotechnical and Geoenvironmental Engineering. 141 (2015) 04015016. https://doi.org/10.1061/(ASCE)GT.1943-5606.0001295.

[6] T. Başer, Y. Dong, A.M. Moradi, N. Lu, K. Smits, S. Ge, D. Tartakovsky, J.S. McCartney, Role of nonequilibrium water vapor diffusion in thermal energy storage systems in the vadose zone." Journal of Geotechnical and Geoenvironmental Engineering. 144 (7): 04018038. https://doi.org/10.1061/(ASCE)GT.1943-5606.0001910.

[7] T. Baser and J.S. McCartney, Transient evaluation of a soil-borehole thermal energy storage system, Renewable Energy 147, 2582-2598.

[8] J. Gao, X. Zhang, J. Liu, K.S. Li, J. Yang, Thermal performance and ground temperature of vertical pile-foundation heat exchangers: A case study, Applied Thermal Engineering. 28 (2008) 2295–2304.

[9] A. Zarrella, M. De Carli, A. Galgaro, Thermal performance of two types of energy foundation pile: Helical pipe and triple U-tube, Applied Thermal Engineering. 61 (2013) 301–310. https://doi.org/10.1016/j.applthermaleng.2013.08.011.

[10] B. Bezyan, S. Porkhial, A.A. Mehrizi, 3-D simulation of heat transfer rate in geothermal pile-foundation heat exchangers with spiral pipe configuration, Applied Thermal Engineering. 87 (2015) 655–668. https://doi.org/10.1016/j.applthermaleng.2015.05.051.

[11] H. Park, S.-R. Lee, S. Yoon, J.-C. Choi, Evaluation of thermal response and performance of PHC energy pile: Field experiments and numerical simulation, Applied Energy. 103 (2013) 12–24. https://doi.org/10.1016/j.apenergy.2012.10.012.

[12] COMSOL Multiphysics, Subsurface Flow Module User's Guide, (2018).

[13] M.T. van Genuchten, A closed-form equation for predicting the hydraulic conductivity of unsaturated soils 1, Soil Science Society of America Journal. 44 (1980) 892–898.

[14] Y. Mualem, A new model for predicting the hydraulic conductivity of unsaturated porous media, Water Resources Research. 12 (1976) 513–522. https://doi.org/10.1029/WR012i003p00513.

[15] T. S. O. Morais, C. H. C. Tsuha, In-situ measurements of the soil thermal properties for energy foundation applications in São Paulo, Brazil, Bulgarian Chemical Communications. 50 (2018) 34–41.